frontiers in Materials

ORIGINAL RESEARCH
published: 29 January 2021
doi: 10.3389/fmats.2020.624791

Char Products From Bamboo Waste Pyrolysis and Acid Activation

Prakash Parthasarathy[1]*, *Hamish R. Mackey*[1], *Sabah Mariyam*[1], *Shifa Zuhara*[1], *Tareq Al-Ansari*[1,2] *and Gordon McKay*[1]

[1]*Division of Sustainable Development, College of Science and Engineering, Hamad Bin Khalifa University, Qatar Foundation, Doha, Qatar,* [2]*Division of Engineering Management and Decision Sciences, College of Science and Engineering, Hamad Bin Khalifa University, Qatar Foundation, Doha, Qatar*

Bamboo is found worldwide but is especially concentrated in tropical and subtropical areas with the major producing nations being China, Indonesia and Thailand with an annual production of 12 million tonnes. It has found uses in many applications such as: furniture, flooring, roofing, fencing, interior design and scaffolding in the construction industry. In this study, discarded waste bamboo furniture was used in the ground form as the raw material feedstock for the production of a series of biochars and activated carbons. The biochars were produced at different temperatures, namely, 723, 823, 923, 1,023, 1,123 and 1223 K, in a muffle furnace inerted with nitrogen and for different pyrolysis times. The product chars yields were 20–30% by weight of the raw material, surface areas were 100–350 m^2/g. Other tests include elemental analysis, helium displacement density, pH, ICP-AES on a leachate sample. Four of the different temperature samples of biochar were used to adsorb the basic dye methylene blue and were shown to possess high adsorption capacities. Then, the same bamboo raw material powder was treated with acid and pyrolysed/activated in a nitrogen atmosphere at the same range of temperatures to produce activated carbons; these were characterized using similar test methods to the biochars. The yields are in the range 20–40% by weight of the raw material feedstock and the BET surface areas are in the range 200–600 m^2/g. Three of the different temperature activated carbons were used to adsorb methylene blue and the results were compared with the biochar results. All the adsorption experimental isotherm results were analyzed using conventional isotherm equations. The benefits and cost implications of both biochar and activated carbon routes are discussed. The methylene blue adsorption capacities are extremely attractive in the range 0.42–1.12 mmol/g (150–300 mg/g char product) and extend to over 2.35 mmol/g (700 mg/g) for the bamboo derived activated carbons. The micropore and mesopore volumes have been determined under the various char and activated carbon experimental conditions and coupled with the surface areas; these results have been used to explain the trends in the methylene blue adsorption capacities.

Keywords: bamboo char, bamboo activated carbon, pyrolysis, characterization, dye adsorption

OPEN ACCESS

Edited by:
Weigang Zhao,
Fujian Agriculture and Forestry University, China

Reviewed by:
Rock Keey Liew,
Universiti Malaysia Terengganu, Malaysia
Xiaofei Tan,
Hunan University, China

***Correspondence:**
Prakash Parthasarathy
pparthasarathy@hbku.edu.qa
prakrock@gmail.com

Specialty section:
This article was submitted to Carbon-Based Materials, a section of the journal Frontiers in Materials

Received: *01 November 2020*
Accepted: *23 December 2020*
Published: *29 January 2021*

Citation:
Parthasarathy P, Mackey HR, Mariyam S, Zuhara S, Al-Ansari T and McKay G (2021) Char Products From Bamboo Waste Pyrolysis and Acid Activation. Front. Mater. 7:624791. doi: 10.3389/fmats.2020.624791

INTRODUCTION

Bamboo is one of the most rapidly growing species of woody materials; it falls under the woody-grasses family of Bambusoideae covering 75 genera and 1,250 species worldwide (Scurlock et al., 2000). Although growing worldwide, it is found more concentrated in tropical and subtropical regions spreading across various continents apart from Europe. The top leading producers being China, India, Myanmar, Thailand, Indonesia, Bangladesh, Vietnam, and South Korea producing about 12 million tonnes annually (The State of the World's Forests 2018, 2018). Bamboo has very low nitrogen, sulfur, and ash contents, which render it attractive in many applications, such as clothing, fencing, food, furniture, flooring, interior design, roofing, and especially in construction and for scaffolding in the construction industry (Bambooz, 2020). As a result of these widespread applications of this rapidly growing sustainable material, thousands of tonnes of waste bamboo is disposed of by landfilling each year (Mui et al., 2008). The bamboo tubes cause major problems to landfill operators as the air and gases in the hollow rods expand and cause a lifting of the landfill resulting in a significant disturbance to the site. Above ground storage results in air and water filled tubes which attract insect infestations such as mosquitoes. Consequently, the bamboo rods are shredded at considerable energy expense prior to safer and more secure landfilling.

The thermal treatment of waste bamboo into char and activated carbon products, especially for water treatment applications has generated considerable interest in the past twenty years (McKay, 1996; Yang, 2003). Water treatment by adsorption has been employed as a separation and purification process commercially since a long time. Adsorbents which are highly porous and possessing good selectivity such as activated carbons are proven to be very effective in removing organic compounds such as dyes (Derbyshire et al., 1995; Choy et al., 2004).

There are plenty of adsorbents in laboratory and commercial use, some being carbon (Cesano et al., 2019), activated carbon (Rodriguez-Reinoso and Ramirez, 2013), silica gel (McKay et al., 1980), zeolites (Liu et al., 2014), and activated alumina (Wasti and Ali Awan, 2016). A few other examples are as follows-bone char (Ko et al., 2005), agricultural residues/by-products, such as:- woodmeal (Rosas et al., 2014; Litefti et al., 2019), nutshells (Torres-Pérez et al., 2015), palm kernel shell (Su et al., 2020), bagasse (Valix et al., 2004), rice straw (Hameed and El-Khaiary, 2008), fruit stones (Lam et al., 2018a), maize cob (Müller-Hagedorn and Bockhorn, 2007), mushroom waste (Lam et al., 2018b), inorganic minerals, such as, montmorillonite (Fil et al., 2012), halloysite (Yuan et al., 2015), layered double hydroxides bentonite (Mockovčiaková and Orolínová, 2009), Fuller's Earth (Subba Reddy et al., 2018), and clays (Lee and Tiwari, 2012); natural materials, including peat (Sepulveda et al., 2008), lignite (Choy et al., 2005), seafood waste-derived chitosan (Alyasi et al., 2020), and chitin (Ilnicka and Lukaszewicz, 2015). These materials have been used for cleaning up polluted water; plastic wastes and biomass gasification residues to chars and activated carbon are also attracting a lot of attention (Bazargan et al., 2013; Benedetti et al., 2019). Of late, some new adsorbent materials such as graphenes (Kyzas et al., 2018; Abu-Nada et al., 2020), carbon nanotubes (Gupta et al., 2013), MCM-41 (Lam et al., 2007), schwartzites (Boonyoung et al., 2019) have also been reported in the literature as high capacity adsorbents.

The choice of the adsorbent material in the application of adsorption processes is mainly based on the uptake potential (capacity), the ability to be re-used and regenerated, and economics of the contact system design and adsorbent material. An ideal adsorbent should meet four essential criteria (Do, 1998; Hadi et al., 2015a, Hadi et al., 2015b) and the textural properties should be complementary to the adsorbate-adsorbent system (Valix et al., 2006; Ruiz-Rosas et al., 2019):

(1) reasonably high surface area, normally present as micropore or small mesopores volume, containing a large number of compatible activated sites,
(2) relatively large porous network for diffusion;
(3) an ability to be regenerated and re-used;
(4) low-cost.

In the case of dyestuffs loaded adsorbents and their regeneration; due to the refractory nature of many dyestuffs, complex and costly thermal regeneration is necessary, resulting in a 5–10% loss in adsorbent weight. Consequently, a high adsorption capacity and low adsorbent cost become the significant factors. For a high capacity, the quantity of active sites directly depends on the surface area, or specifically, the micropore/tiny mesopore volume which significantly contributes to the surface area (Al-Degs et al., 2005), hence an adsorbent material with a high surface area is beneficial in these cases. A decent large porous complex network is also advantageous as it aids for a higher diffusion rate which is vital for the process design of the system and adsorption kinetics.

There are a few studies based on physical activation which were carried out to assess the prospect of employing lignocellulosic materials such as bamboo, fruit stones in the synthesis of cheap adsorbents. Asada et al. (2002) produced bamboo charcoal conducting pyrolysis experiments at temperatures ranging 773–1273 K under an inert atmosphere of nitrogen (Asada et al., 2002). The generated charcoal was then tested for removing some gas contaminants such as benzene, ammonia, toluene, and some indoor volatile organic carbons (VOCs). The study demonstrated that the surface area of char increases with carbonization temperature. Further, it was observed that the resulting chars were displaying surface areas upto 491 m^2/g which are considered moderately high. Benzene and toluene removal efficiencies were the highest for the char produced at 1273 K, but the removal efficiency for ammonia adsorption was a maximum on bamboo carbonized at 773 K, suggesting the formation of an acidic functional group, such as carboxyl at the lower carbonization temperatures. In another study, Mizuta et al. (2004) produced bamboo char performing carbonization experiments at 1173 K for 1 h. The produced char displayed a surface area of 400 m^2/g and was tested for the removal of moderate nitrate-nitrogen (Mizuta et al., 2004). Kim et al. (2006) pyrolyzed bamboo to 973 K for 2 h and the

resultant char showed a micropore volume and surface area of 0.108 cc/g and 247 m^2/g respectively (Kim et al., 2006). This char was subsequently impregnated in KOH for further activation, producing highly porous electrodes (surface area 1,000 m^2/g+) for electric double layer capacitor. Qi et al. (2006) pyrolyzed bamboo in a fixed-bed pyrolyzer (reactor) at temperatures between 623 and 873 K for 10 h (Qi et al., 2006). The yield of char decreased sharply from 34% at 623 K to 30% at 723 K and beyond that value there was no significant difference (<1.5%) in the yields observed at higher temperatures up to 873 K. A study by Jung et al. (2008) using a fluidized bed pyrolyser confirmed this result and claimed that the pyrolysis was essentially completed at 673 K (Jung et al., 2008). While, Wang et al. (2008) carbonized bamboo in nitrogen at 1173 K for 2 h. The yield of char was 25.8% and the char was found to exhibit surface areas up to 564 m^2/g. The produced chars were then used to remove Cu^{2+}, Pb^{2+}, and Cr^{6+} in the concentration range 8–10 ppm (Wang et al., 2008).

In the present study, discarded waste bamboo furniture has been shredded and used as a raw material feedstock. The shredded bamboo powder was pyrolyzed to produce bamboo biochars at different temperatures, namely, 723, 823, 923, 1,023, 1,123 and 1223 K, in a muffle furnace inerted with nitrogen at different reaction times. The product chars were analyzed for yields, surface area, elemental analysis, helium displacement density, pH, ICP-AES on a leachate sample. Three of the different temperature samples of biochar were used to adsorb the basic dye methylene Blue (MB) and were shown to possess high adsorption capacities. Then, the bamboo powder was treated with acid. The purpose of using acid activation is two-fold, firstly to minimize the ash content in the biochar and activated carbon products by removing soluble silica; and, secondly, to produce activated carbons with a highly active surface containing a high content of acidic functional groups containing–carboxylic, lactonic and phenolic groups. In this particular instance, acidic functional groups are targeted to attract the positively charged methylene blue ions. The powder was then pyrolyzed/activated in a nitrogen atmosphere at the same range of temperatures to produce activated carbons; these were characterized using similar test methods to the biochars.

MATERIALS AND METHODS

Material

Raw untreated bamboo was procured from discarded bamboo furniture at a local warehouse. The collected bamboo was then washed with de-ionized water and subsequently crushed into powder. The powder was then segregated into different particle sizes using sieves. The size faction of bamboo used all through the study was 355–500 μm. Several characterisation tests were performed.

Thermogravimetric Analysis

The thermal behavior of the bamboo powder was studied using a Thermogravimetric analyser (TGA/DTA 92, Setaram). The thermal analysis was carried out under an N_2 atmosphere (ultra-high purity 99.999%) of flowrate 180 ml/min at different heating rates. The analysis was performed in triplicate and approximately 10–12 mg sample was placed into a platinum holder connected to a precise balance having a sensitivity of 1 μg. The change in weight of the sample was recorded by a series of light and photocells with a magnet and moving coil system.

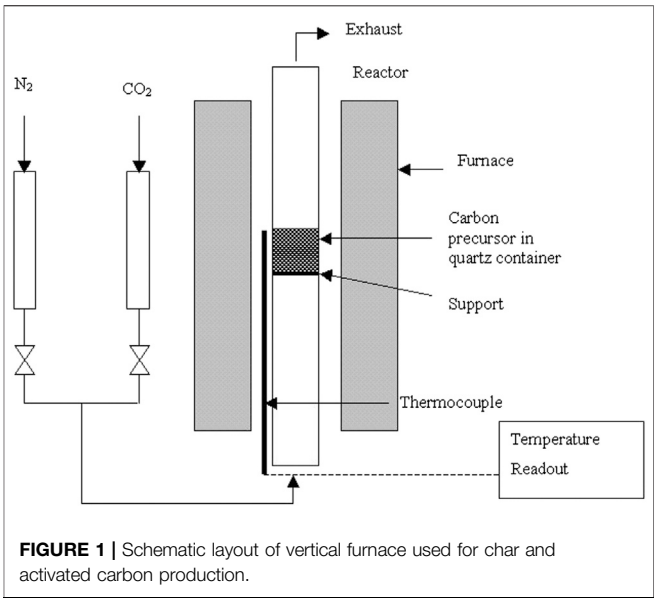

FIGURE 1 | Schematic layout of vertical furnace used for char and activated carbon production.

Carbonization and Activation

The bamboo pyrolysis and activation was conducted using a muffle furnace (AAF 11/18, Carbolite) of capacity 18 L. The furnace was purged with nitrogen (99.99%+ purity) flowing at a rate of 200 ml/min. The furnace was controlled by an PID controller with an adjustable heating rate. All the experimental runs were performed at a uniform heating rate of 5 K/min. Before the commencement of each run, the whole system (furnace and gas line) was inerted with N_2 for about 30 min to remove residual air from the system. Once the desired set temperature was reached, the system was cooled by passing nitrogen until the temperature of the furnace falls below 373 K. To prevent moisture adsorption by the samples, the crucibles were protected with lids and stored in a dessicator.

A 10 g of dried bamboo was washed with concentrated H_2SO_4 (98% w/w). Four samples were prepared using different impregnation ratios of 1, 2, 3, and 4. The sample mixtures were stirred continuously until no further fuming and agitation was seen. Then, they were dried using a muffle furnace at 378 K for about 12 h. The process schematic for both pyrolysis and activation is shown in **Figure 1**.

The bamboo, dried acid-impregnated bamboo samples were heated to the set temperature at a heating rate of 5 K/min under an N_2 atmosphere (99.99% purity) in a Carbolite muffle furnace (model 12/75/700). The sample was maintained at the set temperature for about 1–4 h and was cooled supplying nitrogen until the temperature drops below 378 K. The sample was then taken to a desiccator and was allowed to cool further. The cooled sample was put in a beaker containing 500 ml of

deionized water and the mixture was stirred for about 4 h. Then, the mixture was filtered using a glass-fibre membrane (GC-50, diameter 45 mm, Advantec) and the collected filtrate was repeatedly rinsed with deionized water until it reached a pH of 5.5. The filtrate was then dried in an oven maintained at 378 K for about 12 h, the dried carbon was re-weighed and preserved for subsequent analyses.

Characterization of Chars and Activated Carbons

Surface Area and Pore Size Distribution

The surface area and pore size distribution can be correlated using gas adsorption at the equilibrium partial pressure (P/Po) maintained at a constant temperature. In this study, approximately 0.1 g representative sample was outgassed at a temperature of 573 K for about 6 h. The outgassing was then succeeded by nitrogen sorption in a Coulter SA-3100 surface analyser at 77 K. The monolayer adsorbed gas capacity (Vm) of the sample was determined from the volume adsorbed (V) through the BET, Brunauer et al. (1938) **Eq. 1** (Brunauer et al., 1938).

$$\frac{1}{V[(Po/P)-1]} = \frac{C_{BET}-1}{V_m C_{BET}}\left(\frac{P}{Po}\right) + \frac{1}{V_m C_{BET}} \quad (1)$$

where CBET is known as BET-constant and Vm is the monolayer adsorbed gas capacity.

The specific surface area per unit mass is evaluated by the **Eq. 2**:

$$S_{BET-N_2} = q_m N_A A_m \quad (2)$$

where $S_{BET\text{-}N2}$ denotes the BET surface area (m^2/g); q_m represents the quantity of nitrogen adsorbed in the monolayer (mol/g), N_A is Avogadro number which equals 6.023×10^{23} (molecules/mol), and A_m denotes the projected area of a nitrogen molecule (16.2×10^{-20} m^2 at 77 K).

The t-plot method (Lippens and de Boer, 1965; Gregg and Sing, 1982) was employed to determine the micropore volume, which is a function of the statistical thickness, t (Å), determined by the Harkins and Jura (1944) **Eq. 3** (Harkins and Jura, 1944):

$$t = \left[\frac{13.99}{0.034 - \log(P/Po)}\right]^{0.5} \quad (3)$$

In the assessment of mesopore (or external) surface area and volume, the Kelvin equation (Gregg and Sing, 1982) was adopted on the assumption that Kelvin equation is applicable over the complete mesopore range (Rouquerol and Sing, 1999). The mesopore volume can be determined by a graphical method which is based on the difference between the cumulative volume at the pore size width of 50 nm and 2 nm. The cumulative/total pore volume is the sum of micro and mesopore volume. In other words, it is the volume of nitrogen that is adsorbed at ~ 0.96 P/Po.

Elemental Composition

An elemental analyser (Vario EL III, Varian) was employed to evaluate the composition of carbon, nitrogen, hydrogen, and sulfur present in the sample. A sample of known weight was taken in a capsule and was oxidized at 1673 K. The obtained gas mixture containing N_2, CO_2, H_2O, and SO_2 was passed into a set of adsorption columns connected with a thermal conductivity detector (TCD). The composition of elements was then evaluated by estimating the variance in the electrical conductivity between helium (standard reference, ultra-high purity, 99.999%) and reaction gas. The composition of oxygen was calculated by difference.

Helium Displacement Density

The solid density or helium displacement density was measured using an ultrapycnometer (UPY-1000, Quantachrome) which works based on Archimedes' principle and ideal gas law of fluid displacement. In this analysis, helium gas of purity 99.999% was used as the working fluid. It was interesting to note that the helium (displaced fluid) could penetrate into even tiny pores of diameter 25 nm. The true density of the sample is estimated by calculating the difference in volume before and post helium displacement.

Ash Content

A muffle furnace was employed to determine the ash content of the sample and ASTM D2866-04 (ASTM, 2005) was used for the analysis. The analysis involved taking an accurately weighed sample of 0.8–1.0 g and heating it to 923 ± 25 K for 4 h. After cooling, the crucible with ash was reweighed and the weight of ash alone was determined. The ash content is given as the composition (%) of weight of ash to the initial weight of the sample.

pH

The pH of the sample was determined using a modified ASTM standard method D3838-99 (ASTM, 2005). About 1 g of dried sample was put into a beaker containing 10 ml of boiling deionized water. The solution mixture was heated and allowed to boil for about 15 min in a sealed tube. Then, the solution was filtered employing a pre-moistened filter paper (Whatman No. 2, 110 mm diameter). The pH of the filtrate that was obtained at 323 ± 5K was considered as the sample pH.

Adsorption Isotherm Studies

Dyes

A basic dye MB was used in these studies. The characteristic properties of the dye are Color Index (CI) 52,015, molecular weight in g/mol is 319, percentage dye content is 97%, wavelength for maximum absorption, λmax = 661 nm, and the charge on the colored ion is +1; the molecular structure and estimated dimensions are shown in **Figure 2**.

The molecular structure diagram indicates a minimum molecular dimension for MB of: 1.69 (Length) × 0.70 (Width) × 0.39 (Height). The units are in nm.

Equilibrium Contact Time for Adsorption

The equilibrium contact period was calculated by allowing a definite mass of adsorbent to be in contact with the MB dye stock solution at a fixed concentration of 1,000 ppm. For each carbon,

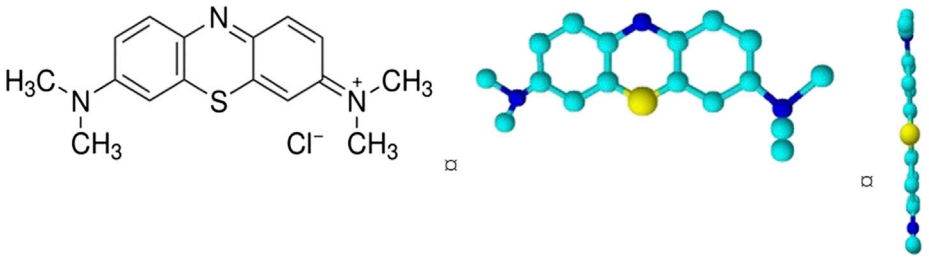

FIGURE 2 | Molecular structure of MB (Basic Blue 9).

five bottles of fixed volumes (50 ml) of solutions with known dye concentrations were made into contact with known weight of carbons (0.05 g), *i.e.*, mass/volume ratio was 1. The bottles were sealed and agitated in a thermostatted shaker bath supplied by Gallenkamp, United Kingdom, at the speed of 200 rpm. On day 1, 2, 3, 4, and 5 after the commencement of the run, one bottle was withdrawn from shaking. The mixtures were filtered, diluted, and analyzed by UV-Vis spectrophotometry. Equilibrium was achieved in 24 h, so the isotherm studies were performed for 2 days to ensure equilibrium was achieved.

Equilibrium Isotherm

A sample of known weight say 0.05 g was taken and 50 ml dye solution of various concentrations ranging from 0.10 to 3.5 mmol/L was added to it. The bottles covered with seals were agitated in a thermostatted shaker (Gallenkamp, United Kingdom) at 200 rpm for 10 days. After shaking, 0.22 μm syringe filters (Millex GP, Millipore) were employed to filter the mixtures. The filtrates were then washed with deionized water and examined using UV-Vis spectrophotometer (Cary 1E, Varian).

The single-dye concentration (C) before and after adsorption was measured using UV-Vis spectrophotometry. The measurement was done based on Beer-Lambert's Law, shown in **Eq. 4**, which states that concentration is linearly related to the absorbance of the UV-light passing through the sample at a specified wavelength:

$$C = \frac{O_d}{\varepsilon \times z} \tag{4}$$

where C is the dye concentration (ppm); Od is the optical density (dimensionless); ε is a molar absorptivity constant and z is the path length of UV-light passing through (m).

RESULTS AND DISCUSSION

Production and Characterization of Bamboo Chars

The results of the elemental analysis are: carbon 51.7%; hydrogen 5.20%; oxygen 41.7%; nitrogen 0.05%; sulfur 0.05%; and ash 0.80%.

Wet chemical analysis confirms that as like other plant biomass bamboo is also composed of cellulose, hemicellulose, lignin, pentosan, and traces of ethanol extractives (Azeez and Orege, 2018; Wang et al., 2020). Detailed classification further divides these components into different types of polysaccharides. This analysis was not performed in this study but a typical set of results for dried bamboo are: ethanol extractives 1.5%; lignin 26.2%; glucan 43.3%; xylan 24.6%; mannan 0.6%; arabinan 1.2% and galactan 1.3% (Scurlock et al., 2000).

Effect of Temperature

Figure 3 presents the effect of pyrolysis on the weight loss fraction of the raw bamboo. **Table 1** presents the effect of temperature on the yield of char at a residence time of 2 h. It can be noted from the table that the yield of char decreased when the temperature was increased from 623 to 1223 K. Around 573 K, some components of bamboo did not undergo pyrolysis and the decomposition is incomplete. At this temperature, a significant quantity of bamboo remains as solid residue (Lam et al., 2018a). However, when the temperature was raised from 673 to 723 K, a significant reduction in the char yield was observed. This drastic decrease could be due to the decomposition of hemicellulose and cellulose which had degraded at 523 and 623 K respectively. Around 673 K, both hemicellulose and cellulose could have been transformed to stabilized char and gas constituting CO, CO_2, H_2O, and CH_4 (Gaur and Reed, 1998; Banyasz et al., 2001; Molina-Sabio and Rodriguez-Reinoso, 2004; Strezov et al., 2007). A further decrease in char yield from 723 K could have been due to the degradation of lignin. The lignin degradation contributed to the decrease in char yield from 27.9 (723 K) to 22.9% (1223 K).

The relationship between C, H, and O with respect to temperature is illustrated in **Figure 4**. This figure shows the trends of how the H/C and O/C change, due to the effect of different pyrolysis temperatures. At high temperatures, a decreasing trend in H/C vs. C/V occurs indicating that the occurrence of char aromatization which follows the heat-up phenomena (Sharma et al., 2001; Fierro et al., 2007). A high correlation coefficient ($R^2 > 0.85$) indicates that reactions other than dehydration could have taken place during the course of pyrolysis (Puziy et al., 2005). The H/C ratio was high (0.5) at low pyrolysis temperature of 673 K indicating a significant presence of organic matter which could have been lignin and cellulose residue. This matches with the findings of Chun et al. (2004), who noted that the cereal residue char was displaying a high H/C ratio of ~0.55 and inferred that the char possessed a substantial quantity of organic matter such as cellulose (Chun et al., 2004).

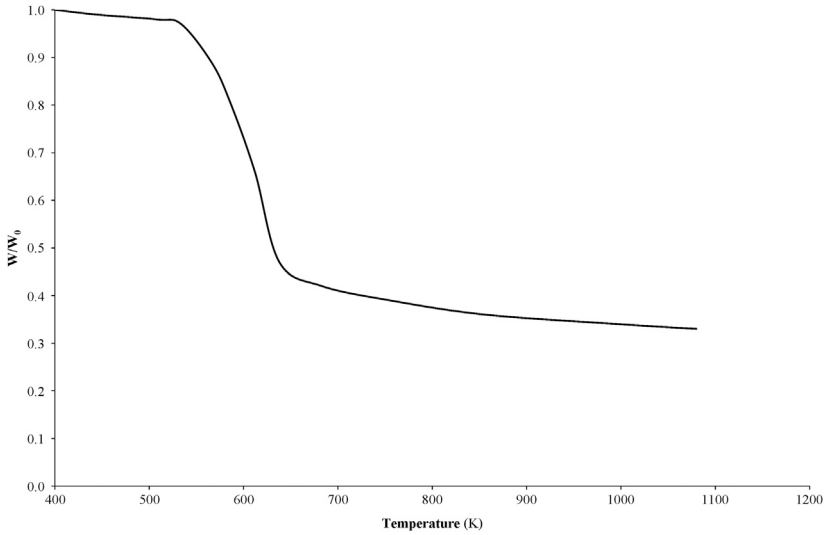

FIGURE 3 | Thermogravimetric analysis on bamboo (heating rate: 5 K/min).

TABLE 1 | Effect of temperature on the elemental composition of chars from bamboo.

Temp. (K)	Yield (%)	Elemental composition					Ash (%)
		N	C	S	H	O*	
623	32.65	0.35	67.06	0.18	3.00	23.85	5.56
723	27.92	0.31	71.72	0.32	2.55	18.00	7.10
823	26.55	0.29	72.58	0.43	2.40	17.05	7.25
923	25.21	0.33	73.23	0.54	2.30	16.25	7.35
1,023	24.02	0.35	73.30	0.61	2.04	15.45	8.25
1,123	23.37	0.37	74.06	0.68	1.55	14.22	9.12
1,223	22.86	0.38	74.83	0.78	1.20	13.26	9.55

**Oxygen content as determined by difference.*
Note: Data values are the average values of 3 experiments within ±6.5%.

Table 2 presents the textural properties of bamboo char that was prepared at 5 K/min heating rate and was held at the set temperature for 2 h. It can be seen from the table that increase in temperature effected an increase in the size of the pores. From 623 to 723 K, the decrease in weight loss of the sample was attributed to the decomposition of hemicellulose and cellulose. The pore development in the char due to lignin is limited as it degrades only after 723 K. This is well supported by the low total pore volume of 0.073 cm^3/g observed at small temperatures.

When the temperature was increased further from 723 to 923 K, the yields of char reduced drastically however the impact was not that much effective as it happened in the development of porosity. The available heat at these temperatures did not support much for the conversion of lignin into char, nonetheless it favored a significant increase in the surface areas. The degradation of lignin initiated only after 1023 K. At temperatures above 1023 K, pores especially micropores developed which can be ascribed to the evolution of volatiles. The surface area of the char improved from 228 to 350 m^2/g when the temperature was elevated from 1023 to 1223 K. The total pore volume also increased from 0.133 to 01.97 cm^3/g for the above temperature range. The above values (surface area and total pore volume) are much higher than the values of chars produced at 823 K (140.2 m^2/g and 0.085 cm^3/g). The bamboo char solution pH values were in the range 6.2 ± 0.3.

Upon increasing the temperature to 1223 K, the burn-off rate decreased since there was no appreciable quantity of volatiles left in the char. The production of new pores was restricted and the pore development in this stage moved to pore widening wherein a portion of micropores was becoming enlarged to mesopores which can be ascribed to the burn-off of carbon molecules at prevailing pore entrances. In this stage, the formation of new pores reduced while the development of pores occurred extensively. Widening of pores took place wherein micropores developed to mesopores. This development can be ascribed to the burn-off of the carbon particles which exists at the pore entrances. It is interesting to note that at this temperature (1223 K), the surface area (350.0 m^2/g) and micropore volume (0.197 cm^3/g) of char was maximum.

Effect of Holding Time

The influence of holding time on the elemental composition of chars produced at 1223 K and 5 K/min heating rate is presented in **Table 3**. It can be seen that with the increase in holding time, the yield of char decreased marginally. The yield that was 23.20% at 1 h holding time decreased to 20.22% at 4 h. The increase in the holding time also decreased the composition of carbon, hydrogen, and nitrogen which can be ascribed to burn-off of carbon. The chars obtained at 1223 K could have been primarily due to carbonized lignin as cellulose and hemicellulose could have decomposed at a lower temperature (923 K) (Rodriguez-Reinoso and Molina-Sabio, 1992; Gaur and Reed, 1998; Li et al., 2008). The ash content in the char elevated gradually with increasing time and inorganics present in the ash retained as such.

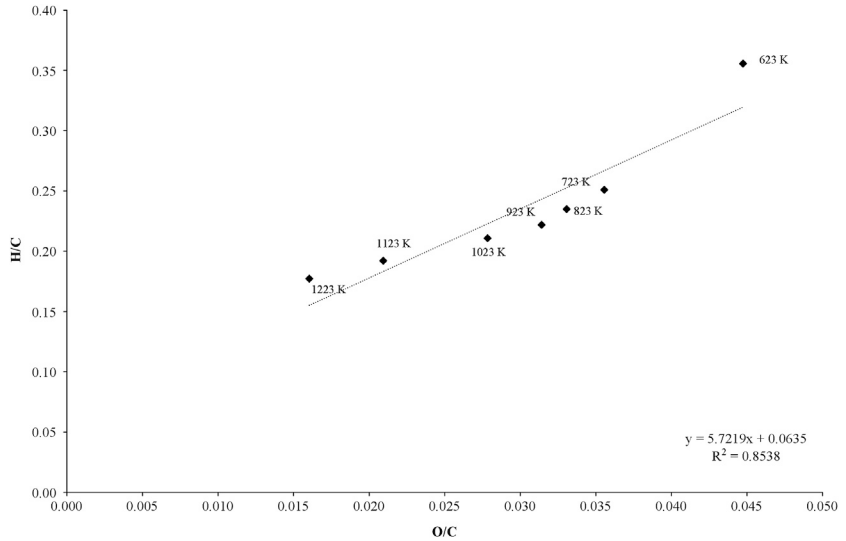

FIGURE 4 | The van Krevelen plot for elemental ratios in bamboo chars prepared at different temperatures.

TABLE 2 | Effect of temperature on textural characteristics on bamboo chars.

Temp. (K)	S_{BET-N2} (m^2/g)	V_{total} (cc/g)	V_{micro} (cc/g)	V_{meso} (cc/g)	ρ_{He} (g/cc)
623	88.5	0.030	0.010	0.020	1.93
723	119.0	0.073	0.024	0.049	1.95
823	140.2	0.085	0.045	0.040	1.97
923	175.1	0.106	0.061	0.045	2.02
1,023	228.5	0.133	0.082	0.049	1.97
1,123	293.6	0.168	0.118	0.050	1.94
1,223	350.0	0.197	0.146	0.051	1.92

Note: Data values are average values of 3 experiments within ±10.0%.

TABLE 3 | Effect of pyrolysis holding time on the elemental composition of chars from bamboo.

Time (h)	Yield (%)	Elemental composition					Ash (%)
		C	H	N	S	O*	
1	23.55	78.75	0.32	0.50	0.39	12.18	7.86
2	22.86	74.83	1.20	0.38	0.78	13.26	9.55
3	21.67	74.10	0.88	0.42	0.30	13.98	10.32
4	20.54	70.52	0.51	0.37	0.28	17.68	10.64

**Oxygen content determined by difference.*

It can be noted from **Table 4** that an increase in residence time from 1 to 2 h produced a positive effect on the surface area and pore volume of the char. This positive effect can be attributed to the increased release of volatiles which have created more pores on the surface of the char particles. Nonetheless, a further increase in the holding from 3 to 4 h effected a reduction in the surface area as well as in the pore volume of the char as a significant portion of volatiles could have been released well before this holding time period. In general, sustainable heating

TABLE 4 | Effect of holding time and heating rate on the textural characteristics of chars from bamboo.

Time (h)	S_{BET-N2} (m^2/g)	V_{total} (cc/g)	V_{micro} (cc/g)	V_{meso} (cc/g)
1	310.0	0.163	0.114	0.049
2	350.0	0.197	0.146	0.051
3	345.5	0.200	0.144	0.056
4	314.4	0.168	0.122	0.046
Heating rate (K/min)	S_{BET-N2} (m^2/g)	V_{total} (cc/g)	V_{micro} (cc/g)	V_{meso} (cc/g)
1	330.8	0.137	0.125	0.012
5	350.0	0.197	0.146	0.051
10	297.9	0.171	0.116	0.050
20	292.3	0.150	0.104	0.046

Note: Data values are average values of 3 experiments within ±10.0%.

(long residence times) alters the structure of carbon atoms wherein contraction of char particles occurs. The contraction of pores reduces the surface area resulting in the collapse of micropores to mesopores (Byrne and Marsh, 1995; Raveendran and Ganesh, 1998).

Effect of Heating Rate

Figure 5 shows the effect of heating rate on the yield of char prepared at 1223 K. It can be observed from the figure the yield of char decreases linearly when the heating rates are increased. This could be due to the temperature gradient that prevails inside the particles which varies with heating rates. As described in slow pyrolysis studies elsewhere (Raveendran and Ganesh, 1998; Demirbas, 2004; Guerrero et al., 2005; Tsai et al., 2007) slow heating rates lead to secondary reactions such as recondensation and depolymerisation.

The issue of tar formation during biomass pyrolysis has received extensive investigation and has been quite successful

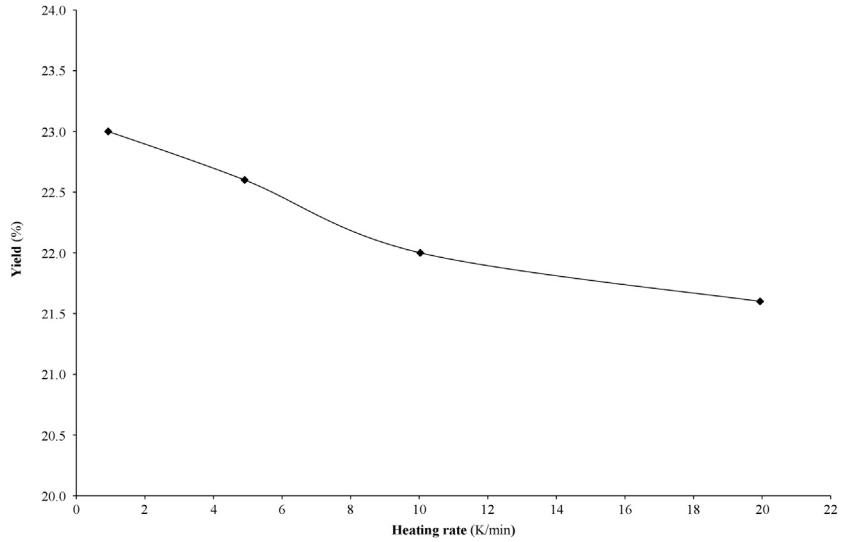

FIGURE 5 | Effect of heating rate to the yield of char from bamboo (N_2, 1223 K, 300–500 μm, 2 h).

TABLE 5 | Effect of particle size to the elemental composition of bamboo chars.

Particle size (μm)	Yield (%)	Elemental composition					Ash (%)
		C	H	N	S	O*	
1,000–2,000	21.60	74.64	0.08	0.35	0.24	16.79	7.91
355–500	22.86	74.83	1.20	0.38	0.78	13.26	9.55

Oxygen content determined by difference.

in order to minimize or eliminate tar production by careful control of the operating conditions. Tars evolved would either undergo cracking into gas phase (Zanzi et al., 2002) or they would remain as carbon particles on the surface of the char thereby increasing the yield of char.

Table 4 illustrates the effect of heating rate on the textural properties of the produced chars. When the heating rate was increased up to 5 K/min, the surface area as well as micropore volume of chars increased. However, when the heating rate was incremented further up to 20 K/min, both surface area and micropore volume decreased. High heating rates create a large temperature gradient inside particles which results in quick polymerization and devolatilization (Haykiri-Acma, 2006). Inconsistent contraction and swelling with volatiles within particles results in the breakdown of the carbon matrix which then results in the closure of pores and reduction in the surface area of the chars.

Effect of Particle Size

The yield and elemental content of chars produced from two particle sizes bamboo powder (1,000–2000 and 355–500 μm) at 1223 K are presented in **Table 5**. It can be observed that the fine particles contributed a slightly higher yield than the large particles.

This could be due to large external surface area (for heat transfer) and shorter diffusion path among particles. Volatiles that comes from the finer particles (355–500 μm) are more prone to undertake secondary reactions wherein the occurrence of tar and reduction of tar endorse extra char production which usually gets retained on the surface of the char particles (Koufopanos et al., 1991; Yang, 2003; Pütün et al., 2005; Bridgeman et al., 2007). This can also be supported by the higher hydrogen content in the char of 355–500 μm in **Table 5**.

Further, finer particles have a smaller temperature gradient than the larger particles (Dupont et al., 2008). Uniform heat distribution reduced the decomposition rate (Sadhukhan et al., 2008; Tonbul, 2008), liberated more water during the degradation of cellulose and hemi-cellulose (Garcia-Perez et al., 2008), hindered contraction and swelling of particles which occurs during the quick release of volatiles. The textural characteristics for these two chars, for 1,000–2000 μm and 355–500 μm, are BET-N_2 surface areas are 320.4 and 350.0 m^2/g respectively and the total pore volumes, VT, are 0.172 (Vmicro = 0.122, Vmeso = 0.0525) and 0.197 (Vmicro = 0.146, Vmeso = 0.0515) cc/g respectively.

Dye Adsorption Potential

So as to evaluate the adsorption potential capacity and characteristics of the bamboo chars, a standard test dye, MB, has been used in the adsorption tests. Due to the large number of chars produced it was not possible to test them all and therefore four isotherms have been performed on the chars produced at the same heating rate of 5 K/min for 2 h at four different temperatures, namely, 923, 1,023, 1,123, and 1223 K. This choice provides the effect of surface area, porosity different surface activation site created at different temperatures.

The four isotherms are plotted in **Figure 6** and the capacities are 0.42 mmol/g char produced at 923 K, 0.51 mmol/g char at 1023 K, 0.86 mmol/g char at 1123 K and 1.12 mmol/g char at 1223 K respectively for a total pore volumes of 0.106, 0.133, 0.168, and 0.197 cc/g respectively. It can be seen that the dye capacity is

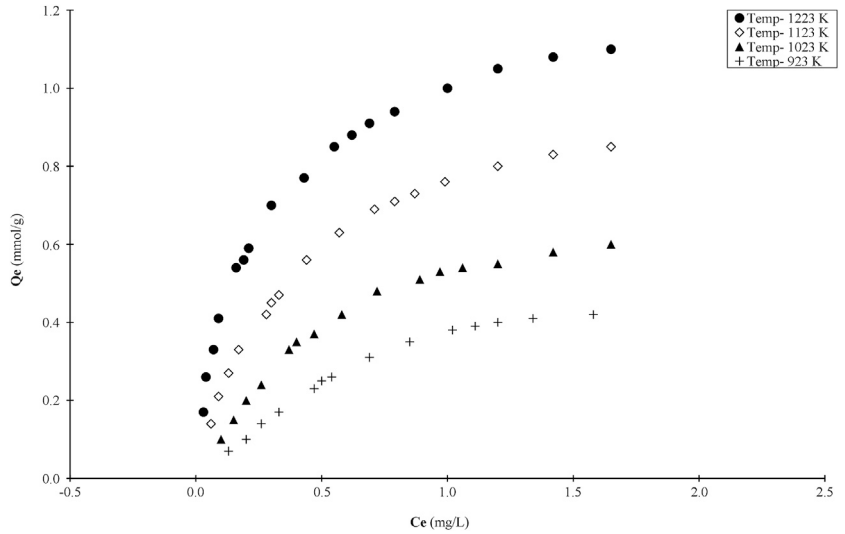

FIGURE 6 | Adsorption curves for MB onto bamboo chars produced at four temperatures (N_2; 2 h, 355–500 μm).

increasing with the increase in total pore volume. The increments are not quite linear because the nature of the surface sites will change with temperature and the relative proportions of micropores to mesopores are also changing.

Production and Characterisation of Bamboo Activated Carbons

Effect of Temperature

Activated carbons have been prepared by the addition of sulfuric acid to the bamboo particles, further details are presented in the experimental and methods *Materials and Methods* section. A sequence of activated carbons was produced from the bamboo particles of size range 355–500 μm and at the temperature of 1223 K; corresponding to the temperature producing the highest surface area and highest MB adsorption capacity char. A sulfuric acid impregnation ratio of 1:1 (Xp = 1) was used in this temperature effect studies. The contact time for all the runs was 2 h as this was shown to give an optimum surface area later. The BET surface areas, the yields and the textural characteristics (surface area, micropore volume, and total pore volume, and) are shown in **Table 6**.

At the higher temperatures the yields are in the range of 20–22% and the microporosity volume steadily increases with temperature and is strongly developed at the high temperatures. The mesopore volume only starts to increase significantly after around 950 K and this is most likely due to the burning away of the micropore walls. The BET nitrogen surface area increases significantly with the increasing temperature reaching a value of 1,106 m^2/g at 1223 K and a total pore volume of 0.562 cm^3/g. All the densities were in the range 2.00 ± 0.05 cm^3/g.

Increasing the activation time decreased the yields considerably and increasing the impregnation ratio also had a significant impact on decreasing the yield. Such an impact can be ascribed to the strong oxidative behavior of H_2SO_4. An increase in the loading ratio from one to four effected a complete decomposition of bamboo components by forming oxygen complexes over the surface of the residues. A relative open porous nature of the residue supported with the improved oxygen complexes induced the liberation of carbon atoms and ultimately effected in the reduction of activated carbon yield. The preferential development of micropores is consistent with the acid intercalation mechanism where it has been suggested that intercalation develops the pores by exfoliating the basal planes in the carbon matrix (Lyubchik et al., 1997; Daulan et al., 1998).

TABLE 6 | Effect of temperature on textural characteristics on sulfuric acid bamboo derived activated carbons (N_2, 2 h, Xp = 1).

Temp. (K)	S_{BET-N2} (m^2/g)	V_{total} (cc/g)	V_{micro} (cc/g)	V_{meso} (cc/g)	Yield % w/w
623	110	0.065	0.020	0.040	35.4
723	152	0.076	0.031	0.045	29.4
823	220	0.112	0.065	0.048	24.8
923	480	0.216	0.141	0.055	23.8
1,023	804	0.421	0.346	0.070	22.0
1,123	986	0.501	0.396	0.105	21.4
1,223	1,106	0.562	0.431	0.131	20.4

Note: Data values are average values of 3 experiments within ±10.0%.

Acid Impregnation Ratio

The effect of the acid impregnation ratio on the activated carbon quality has been investigated at three impregnation ratios, Xp = 1, 2 and 4, at 2 h reaction time, at the high temperature of 1223 K and the BET-N_2 surface areas are 1,106, 820, and 550 m^2/g respectively and the total pore volumes, VT, are 0.562 (Vmicro = 0.421, Vmeso = 0.131), 0.455 (Vmicro = 0.360, Vmeso = 0.095) and 0.250 (Vmicro = 0.190, Vmeso = 0.060) cc/g respectively. The pH values of water containing the bamboo activated carbons were in the range 5.6 ± 0.4.

TABLE 7 | Elemental composition of activated carbons for acid-impregnated bamboo.

Impregnated ratio	Time (h)	Elemental composition (wt%)					Ash (%)
		N	C	S	H	O*	
1	1	0.39	76.96	0.50	2.01	17.19	2.95
	2	0.67	75.32	0.84	1.92	18.20	3.05
	3	0.81	74.98	0.92	1.87	17.66	3.76
	4	0.80	71.68	2.27	1.66	18.19	5.40
4	1	1.81	69.51	2.24	1.24	16.29	8.91
	2	1.56	64.82	2.40	1.22	18.69	11.31
	3	1.49	64.27	2.40	1.22	17.77	12.85
	4	0.88	61.83	2.36	1.21	17.42	16.30

O oxygen content is obtained by difference.*
Note: Data values are average values of 3 experiments within ±10.0%.

Elemental Composition

Table 7 presents the elemental content of activated carbons generated at 1223 K from bamboo powder impregnated with H_2SO_4.

It can be noted that the carbon content of samples decreases with increase in holding time. This decrease can be attributed to the burn-off of carbon which occurred due to the sustained activation at high temperature (1223 K). This phenomenon is also responsible for the reduction of heteroatoms composition such as nitrogen, sulfur, and oxygen. However, oxygen demonstrated an opposite behavior which could be due to the occurrence of oxides in ash following the elimination of carbon atoms.

Different impregnation ratios and time delivered char with different elemental content. It can be noted that an increase in the impregnation ratio decreased the carbon content of chars. At a constant impregnation ratio of 1, when the holding time was elevated from 1 to 4 h, the carbon content reduced from 77.0 to 71.7%. In the other case, at an impregnation ratio of 4, an increase in holding time from 1 to 4 h reduced the carbon content from 69.5 to 61.8%. This indicates that a more intense reaction has occurred between cellulose, hemicellulose, and lignin when the quantity of acid was increased further. As reported by Caballero et al. (1997), H_2SO_4 could have decomposed the 3-D structure of lignin (Caballero et al., 1997). Guo et al. (2005) reported that a high H_2SO_4 often produces undue H_2O content that could burn-off carbons at high temperatures. The reaction of biomass with H_2SO_4 can be expressed as below (Guo et al., 2005).

$$\left[C_n\, H_x\, O_y\right] + H_2SO_4 \rightarrow H_2O + S_{element} + \left[C_nH_xO_{y+3}\right] \quad (5)$$

Activation Holding Time and Heating Rate

The effect of the contact time for activation has been investigated. The normal conditions were undertaken, namely, nitrogen inert gas, 1223 K and an impregnation ratio of 1, Xp = 1, for four different activation times: 1, 2, 3, and 4 h. The BET-N_2 surface area results are 1,029, 1,106, 973 and 849 m^2/g respectively for 1, 2, 3, and 4 h holding time and the adsorption capacities are 2.11, 2.35, 1.82, and 1.41 mmol/g respectively. For impregnation ratios, Xp = 1, 2, 3, and 4, at 2 h reaction time, under the same conditions the total pore volumes, VT, are 0.546 (Vmicro = 0.460, Vmeso = 0.086), 0.562 (Vmicro = 0.472, Vmeso = 0.090) and 0.480 (Vmicro = 0.363, Vmeso = 0.117) cc/g respectively.

It can be observed that increasing time from 1 to 3 h increased the micropore volume. This increase in micropore volume could be due to the intercalation effect of acid which has effected a micropore structure instead of enlarging the pore size. Lyubchik et al. (1997) and Valix et al., (2008) also reported a similar phenomena in acid-treated coal and bagasse respectively (Lyubchik et al., 1997; Valix et al., 2008). Further, H_2SO_4-impregnated activated carbons undergo two mechanisms. When the holding time was incremented from 1 to 3 h, the micropore volumes increased while the acid intercalation developed pores which can be evidenced from the sharp, narrow peaks at 0.7 nm diameter. When the holding time was increased to 4 h, the pores broke down leading to a reduction in the micropore volume and an increment in the micropore volumes. This increase is due to the breakdown of micropore walls.

Dye Adsorption on Bamboo Carbons

The adsorption of MB dye has been performed on the bamboo activated carbons prepared at both different holding times (at a constant temperature of 1223 K) and different temperatures (constant holding time of 2 h) and the experimental results of the isotherm studies at the four higher temperatures are presented in **Figure 7**. The MB saturation adsorption capacities at the four temperatures are: 2.35 mmol/g at 1223 K, 2.04 mmol/g at 1123 K, 1.77 mmol/g at 1023 K and 1.34 mmol/g at 923 K. These are high adsorption capacities and in terms of dye mass 2.35 mmol is equivalent to approximately 750 mg MB dye. Due to the extensive acid treatment, a number of surface group species will be created, for example, carboxylic groups, other acid groups and phenolic groups (Liew et al., 2019). These will dissociate when the adsorbent particles are dispersed in water forming negatively charged carboxylate groups for instance. In water, the methylene blue dye molecules also dissociate into a colored positively charged ion, which is strongly attracted to the carboxylate and other negatively charged sites thus explaining the very high uptake capacity of MB dye.

The bamboo activated carbons exhibit a trend of increasing 'basic' element contents (*i.e.,* nitrogen and sulfur) tending to make the surface charge positive and more attractive to acidic dye species which have a negatively charged colored ion and with a tendency to repel basic dyes, such as MB. Based on the results, there is a slowly decreasing trend with increasing basicity [N + S] indicated in **Table 7** for the adsorption of MB; which is to be expected for the basic dye molecule.

However, the presence of oxygen groups content in the form of $C{=}O^{\delta-}$ suggests that the uptake of MB is attracted to the bamboo carbons. Furthermore, the acidic pH values of the bamboo carbons stated in *Dye Adsorption On Bamboo Carbons* section, reveal that certain parts of the accessible surface also possess some negative charge. This explains partly why the bamboo carbons can adsorb significant amounts of MB even though most bamboo carbons have the sulfur content close to 1% and over.

The dye adsorption capacities are plotted against the micropore volume and total pore volume in **Figure 8** and demonstrate excellent dye uptake values many of which are over 2 mmol dye/g bamboo carbon.

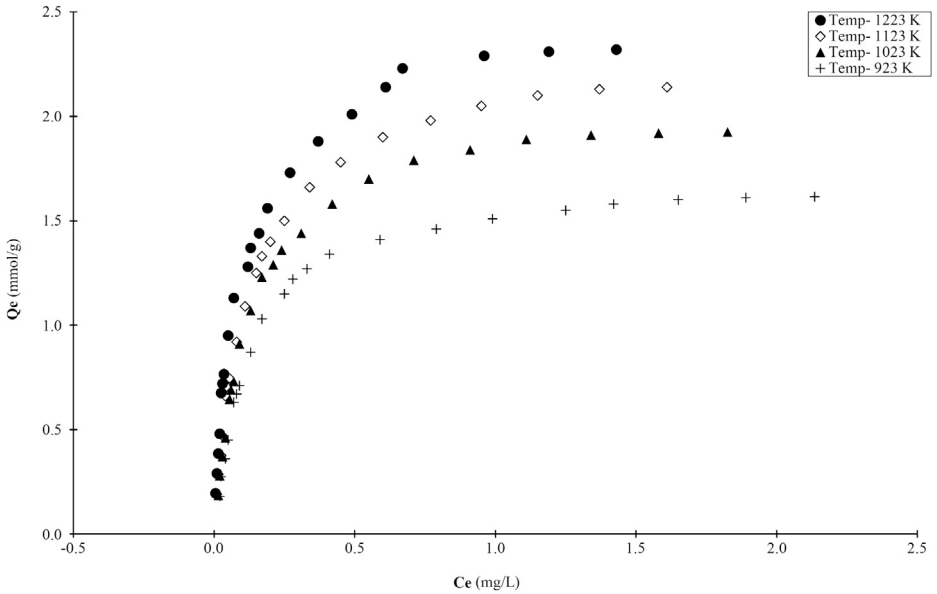

FIGURE 7 | Adsorption curves for MB onto bamboo derived activated carbons produced at four temperatures (N_2; 2 h, 355–500 μm).

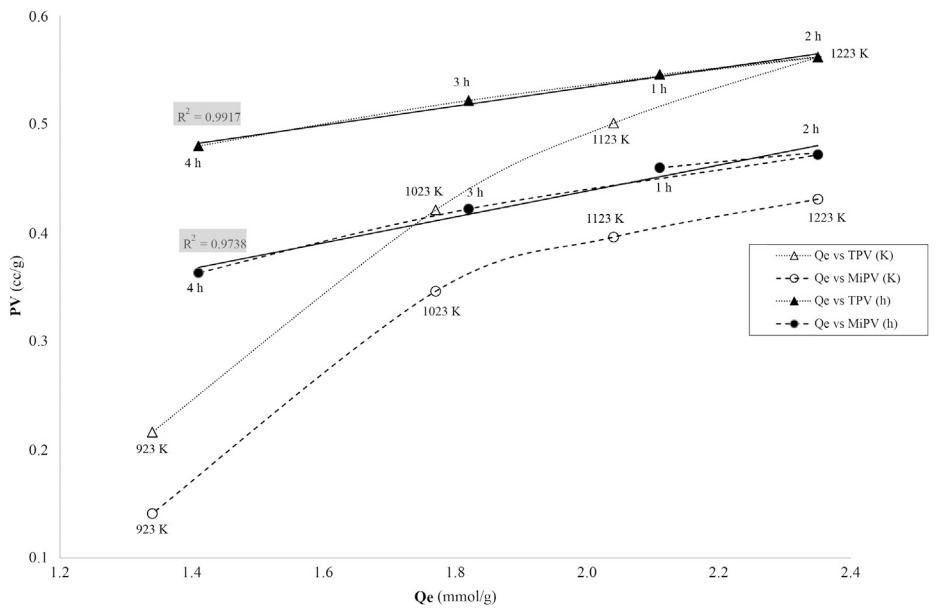

FIGURE 8 | Relationship between amount of MB adsorbed (q_e) and the total pore volume, TVP, and the micropore volume, MiPV, for four activated carbons at different temperatures and the four activated carbons at different holding times.

The dye adsorption capacities are plotted against the pore volume in **Figure 8** and demonstrate excellent dye uptake values. The MB is expected to diffuse into pores with a width larger than 1.5 nm (Cooney, 1999), that is in the large super-micropore zone, when the pore diameter is into sub-region of 1.5–2 nm. The ultra-micropores, $d_p < 0.7$ nm, will not be involved in MB adsorption. The micropore volumes throughout this project were determined by the t-plot method described earlier. Without exception, according to the t-plots, all the carbons have the intercept point on the lnP/Po relationship at film thickness (t) around 0.4 nm that indicates the microporous nature of the carbons.

As shown in **Figure 8**, the dye uptake vs. pore volume (PV) indicates the affinity of MB for the bamboo activated carbon textural properties. The data for the four holding times show a very strong linearity with the total pore volume (TVP) and the micropore

volume (MiPV) having correlation coefficients $R^2 = 0.9917$ and $R^2 = 0.9738$ respectively. Since all these points are at a constant temperature the total pore volume does not undergo a major change, only around 8%. Whereas the effect of temperature will have a significant effect on the TVP, the extent of MiPV vs. the mesopore volume development and also the type of surface active sites. In the case of temperature effect, the pore volume changes are more than doubled and the correlation coefficients for TVP and MiPV are 0.9601 and 0.9016 respectively. The lower R^2 values and the lower capacity values for MiPV are at the two higher temperatures which result in a significant increase in the Vmeso due to the burning of the micropores walls and the subsequent formation of the mesopores. The MB adsorption capacities as a function of VT are very high and for Vmicro also was very high, revealing that MB may be retained in both micro- and mesopores, particularly the super-micropores greater than 1 nm (d_{min} >1.50 nm).

Summarizing, both super-micro- and meso-pore surface areas are involved in the uptake of dye, and this depends on the dimensions/size of the target adsorbate material. For a relatively small dye like MB (pore dmin >1.50 nm), then the TVP volume area correlates well to the amount adsorbed.

Essentially, there are four parameters which affect the adsorption of dye molecules: surface areas of micropores/mesopores, molecular size of the adsorbate, and molecular orientation of the adsorbate and density of specific adsorbent surface heteroatoms such as nitrogen and sulfur for acidic molecules (in the form of $C{=}S^{\delta+}$) and in the case of basic ions/molecules like MB, oxygen (in the form of $C{=}O^{\delta-}$), in which the dimension/size of the adsorbate was considered the most important. With a required pore diameter greater than 1.50 nm for adsorption, MB will adsorb in both the mesopore region and the super-micropore region, in part. The heteroatoms content such as oxygen has been shown to be influential to the surface charge, generating negatively charged surface species such as carboxylic and ketonic groups that affect the bond of the dissociated positively charged dye molecules on to the surface of the carbon particles.

CONCLUSION

The influence of temperature, heating rate, holding time, and particle size to the behavior/characteristics of chars produced from bamboo powder have been investigated. Temperature and holding time are the most critical factors which determine the yields of chars, pore volume, and surface areas. For temperatures between 623 and 1223 K and a 2 h holding time, the yields ranged from 32.65 to 22.86% respectively, the surface areas ranged from 88.5 to 350.0 m^2/g respectively and the porosities ranged from 0.030 to 0.197 cc/g respectively with most of the pore development in the micropore region. A holding time of 2–3 h produced maximum surface area and pore volume. The influence of heating rate and particle size on the char yield is insignificant however their influence on the textural properties of the resultant chars is significant. This can be ascribed to the prevailing temperature gradient of the feedstock while undergoing pyrolysis wherein the extent of shrinkage effects the structure of char. Most volatiles were liberated at 773 K, increasing temperature decreased the yield of char. Carbon chars derived from bamboo show a very reasonable dye adsorption capacity. The maximum uptake of methylene Blue was over 1.1 mmol/g char which is good compared to many chars.

The effects of experimental parameters, such as holding time, acid treatment and impregnation ratio, on the yield as well as textural characteristics and elemental composition were investigated on the production of activated carbon from bamboo at the fixed temperature. For the bamboo activated carbons, produced by activating the char with sulfuric acid, increasing impregnation ratio did not affect the surface area as significantly as holding time. Again, carbons impregnated with sulfuric acid at impregnation ratio (Xp) = 1 had the highest surface area of 1,106 m^2/g (2 h). The MB adsorption capacities of the activated carbons were extremely high and the high surface area carbon just described had an adsorption capacity of 2.35 mmol/g or 750 mg dye/g activated carbon.

There are a number of limitations in the study which could be investigated in future work: it would be interesting to have analyzed various spectra of the materials before and after adsorption to learn more about the mechanisms; it is important to carry out regeneration studies to assess how many times the chars and activated carbons can be used and what adsorption capacity is retained after each regeneration; other activation methods such as using alkali, other acids, microwave activation to see the differences in the characteristic properties would be beneficial; more application studies to remove other types or organic compounds, heavy metal ions, pesticides, endocrine disruptors and other emerging pollutants; tailor-making "designer" chars and activated carbons for each specific application. In terms of food security, assessing which char properties are most appropriate in soil-enhancing agricultural applications.

DATA AVAILABILITY STATEMENT

The raw data supporting the conclusions of this article will be made available by the authors, without undue reservation.

AUTHOR CONTRIBUTIONS

PP: characterisation testing. HM: drafted the activated carbon section of the paper. SM: carried out the char experimental work. SZ: carried out the activated carbon experimental work. TA: drafted the char section of the paper. GM: lead supervisor responsible for project detailing, editing the paper and overall supervision of the paper and the research program.

FUNDING

The authors would like to thank Qatar National Research Fund for their support of this research through NPRP-11S-0117-180328, the Supreme Committee for Delivery and Legacy (SCDL) and to Hamad Bin Khalifa University. Any opinions, findings and conclusions, or recommendations expressed in this material are those of the author(s) and do not necessarily reflect the views of HBKU or QF or SCDL.

REFERENCES

Abu-Nada, A., McKay, G., and Abdala, A. (2020). Recent advances in applications of hybrid graphene materials for metals removal from wastewater. *Nanomaterials* 10, 595. doi:10.3390/nano10030595

Al-Degs, Y. S., El-Barghouthi, M. I., Khraisheh, M. A., Ahmad, M. N., and Allen, S. J. (2005). Effect of surface area, micropores, secondary micropores, and mesopores volumes of activated carbons on reactive dyes adsorption from solution. *Sep. Sci. Technol.* 39, 97–111. doi:10.1081/ss-120027403

Alyasi, H., Mackey, H. R., and McKay, G. (2020). Removal of cadmium from waters by adsorption using nanochitosan. *Energy Environ.* 31, 517–534. doi:10.1177/0958305X19876191

Asada, T., Ishihara, S., Yamane, T., Toba, A., Yamada, A., and Oikawa, K. (2002). Science of bamboo charcoal: study on carbonizing temperature of bamboo charcoal and removal capability of harmful gases. *J. Health Sci.* 48, 473–479. doi:10.1248/jhs.48.473

ASTM (2005). "Refractories, carbon and graphite products," in *Activated Carbon. Annual Book of ASTM Standards* (Easton: ASTM), Vol. 15.01.

Azeez, M. A., and Orege, J. I. (2018). "Bamboo, its chemical modification and products," in *Bamboo - current and future prospects*. Editor H. P. S. Khalil (London, United Kingdom: IntechOpen). doi:10.5772/intechopen.76359

Bambooz (2020). 20 uses of bamboo for home, office and yourself. Available at: http://www.bamboooz.com/20-uses-bamboo/.

Banyasz, J. L., Li, S., Lyons-Hart, J. L., and Shafer, K. H. (2001). Cellulose pyrolysis: the kinetics of hydroxyacetaldehyde evolution. *J. Anal. Appl. Pyrol.* 57, 223–248. doi:10.1016/S0165-2370(00)00135-2

Bazargan, A., Hui, C. W., and McKay, G. (2013). Porous carbons from plastic waste. *Adv. Polym. Sci.* 266, 1–25. doi:10.1007/12_2013_253

Benedetti, V., Ail, S. S., Patuzzi, F., and Baratieri, M. (2019). Valorization of char from biomass gasification as catalyst support in dry reforming of methane. *Front. Chem.* 7, 119. doi:10.3389/fchem.2019.00119

Boonyoung, P., Kasukabe, T., Hoshikawa, Y., Berenguer-Murcia, Á., Cazorla-Amorós, D., Boekfa, B., et al. (2019). A simple "Nano-Templating" method using zeolite Y toward the formation of carbon schwarzites. *Front. Mater.* 6, 104. doi:10.3389/fmats.2019.00104

Bridgeman, T. G., Darvell, L. I., Jones, J. M., Williams, P. T., Fahmi, R., Bridgwater, A. V., et al. (2007). Influence of particle size on the analytical and chemical properties of two energy crops. *Fuel* 86, 60–72. doi:10.1016/j.fuel.2006.06.022

Brunauer, S., Emmett, P. H., and Teller, E. (1938). Adsorption of gases in multimolecular layers. *J. Am. Chem. Soc.* 60, 309–319. doi:10.1021/ja01269a023

Byrne, J., and Marsh, H. (1995). *Porosity in carbons: characterisation and applications*. Editor J. W. Patrick (New York, NY: Halsted Press).

Caballero, J. A., Marcilla, A., and Conesa, J. A. (1997). Thermogravimetric analysis of olive stones with sulphuric acid treatment. *J. Anal. Appl. Pyrol.* 44, 75–88. doi:10.1016/S0165-2370(97)00068-5

Cesano, F., Cravanzola, S., Brunella, V., Damin, A., and Scarano, D. (2019). From polymer to magnetic porous carbon spheres: combined microscopy, spectroscopy, and porosity studies. *Front. Mater.* 6, 84. doi:10.3389/fmats.2019.00084

Choy, K. K., Porter, J. F., and McKay, G. (2004). Single and multicomponent equilibrium studies for the adsorption of acidic dyes on carbon from effluents. *Langmuir* 20, 9646–9656. doi:10.1021/la040048g

Choy, K. K. H., Allen, S. J., and McKay, G. (2005). Multicomponent equilibrium studies for the adsorption of basic dyes from solution on lignite. *Adsorption* 11, 255–259. doi:10.1007/s10450-005-5933-4

Chun, Y., Sheng, G., Chiou, C. T., and Xing, B. (2004). Compositions and sorptive properties of crop residue-derived chars. *Environ. Sci. Technol.* 38, 4649–4655. doi:10.1021/es035034w

Cooney, D. (1999). *Adsorption design for wastewater treatment*. Boca Raton, Florida: CRC Press, Lewis Publishers.

Daulan, C., Lyubchik, S. B., Rouzaud, J. N., and Béguin, F. (1998). Influence of anthracite pretreatment in the preparation of activated carbons. *Fuel* 77, 495–502. doi:10.1016/S0016-2361(97)00202-0

Demirbas, A. (2004). Effects of temperature and particle size on bio-char yield from pyrolysis of agricultural residues. *J. Anal. Appl. Pyrol.* 72, 243–248. doi:10.1016/j.jaap.2004.07.003

Derbyshire, F., Jagtoyen, M., and Thwaites, M. (1995). "Activated carbons – production and application," in *Porosity in Carbons: Characterisation and Applications*. Editor J. W. Patrick (New York, NY: Halsted Press).

Do, D. D. (1998). *Adsorption analysis: equilibrium and kinetics*. London, United Kingdom: Imperial College Press.

Dupont, C., Commandré, J.-M., Gauthier, P., Boissonnet, G., Salvador, S., and Schweich, D. (2008). Biomass pyrolysis experiments in an analytical entrained flow reactor between 1073K and 1273K. *Fuel* 87, 1155–1164. doi:10.1016/j.fuel.2007.06.028

Fierro, V., Torné-Fernández, V., Celzard, A., and Montané, D. (2007). Influence of the demineralisation on the chemical activation of Kraft lignin with orthophosphoric acid. *J. Hazard Mater.* 149, 126–133. doi:10.1016/j.jhazmat.2007.03.056

Fil, B. A., Özmetin, C., and Korkmaz, M. (2012). Cationic dye (methylene blue) removal from aqueous solution by montmorillonite. *Bull. Kor. Chem. Soc.* 33, 3184–3190. doi:10.5012/bkcs.2012.33.10.3184

Garcia-Perez, M., Wang, X. S., Shen, J., Rhodes, M. J., Tian, F., Lee, W.-J., et al. (2008). Fast pyrolysis of oil mallee woody biomass: effect of temperature on the yield and quality of pyrolysis products. *Ind. Eng. Chem. Res.* 47, 1846–1854. doi:10.1021/ie071497p

Gaur, S., and Reed, T. (1998). *Thermal data for natural and synthetic fuels*. New York, NY: Marcel Dekker Inc.

Gregg, S., and Sing, K. (1982). *Adsorption, surface area and porosity*. London, United Kingdom: Academic Press.

Guerrero, M., Ruiz, M. P., Alzueta, M. U., Bilbao, R., and Millera, A. (2005). Pyrolysis of eucalyptus at different heating rates: studies of char characterization and oxidative reactivity. *J. Anal. Appl. Pyrol.* 74, 307–314. doi:10.1016/j.jaap.2004.12.008

Guo, J., Xu, W. S., Chen, Y. L., and Lua, A. C. (2005). Adsorption of NH3 onto activated carbon prepared from palm shells impregnated with H2SO4. *J. Colloid Interface Sci.* 281, 285–290. doi:10.1016/j.jcis.2004.08.101

Gupta, V. K., Kumar, R., Nayak, A., Saleh, T. A., and Barakat, M. A. (2013). Adsorptive removal of dyes from aqueous solution onto carbon nanotubes: a review. *Adv. Colloid Interface Sci.* 193-194, 24–34. doi:10.1016/j.cis.2013.03.003

Hadi, P., Yeung, K. Y., Barford, J., An, K. J., and McKay, G. (2015b). Significance of microporosity on the interaction of phenol with porous graphitic carbon. *Chem. Eng. J.* 269, 20–26. doi:10.1016/j.cej.2015.01.090

Hadi, P., Yeung, K. Y., Barford, J., An, K. J., and McKay, G. (2015a). Significance of "effective" surface area of activated carbons on elucidating the adsorption mechanism of large dye molecules. *J. Environ. Chem. Eng.* 3, 1029–1037. doi:10.1016/j.jece.2015.03.005

Hameed, B. H., and El-Khaiary, M. I. (2008). Kinetics and equilibrium studies of malachite green adsorption on rice straw-derived char. *J. Hazard Mater.* 153 (1–2), 701–708. doi:10.1016/j.jhazmat.2007.09.019

Harkins, W. D., and Jura, G. (1944). Surfaces of solids. Xiii. A vapor adsorption method for the determination of the area of a solid without the assumption of a molecular area, and the areas occupied by nitrogen and other molecules on the surface of a solid. *J. Am. Chem. Soc.* 66, 1366–1373. doi:10.1021/ja01236a048

Haykiri-Acma, H. (2006). The role of particle size in the non-isothermal pyrolysis of hazelnut shell. *J. Anal. Appl. Pyrol.* 75, 211–216. doi:10.1016/j.jaap.2005.06.002

Ilnicka, A., and Lukaszewicz, J. P. (2015). Discussion remarks on the role of wood and chitin constituents during carbonization. *Front. Mater.* 2, 20. doi:10.3389/fmats.2015.00020

Jung, S.-H., Kang, B.-S., and Kim, J.-S. (2008). Production of bio-oil from rice straw and bamboo sawdust under various reaction conditions in a fast pyrolysis plant equipped with a fluidized bed and a char separation system. *J. Anal. Appl. Pyrol.* 82, 240–247. doi:10.1016/j.jaap.2008.04.001

Kim, C., Lee, J.-W., Kim, J.-H., and Yang, K.-S. (2006). Feasibility of bamboo-based activated carbons for an electrochemical supercapacitor electrode. *Korean J. Chem. Eng.* 23, 592–594. doi:10.1007/bf02706799

Ko, D. C. K., Porter, J. F., and McKay, G. (2005). Application of the concentration-dependent surface diffusion model on the multicomponent fixed-bed adsorption systems. *Chem. Eng. Sci.* 60, 5472–5479. doi:10.1016/j.ces.2005.04.048

Koufopanos, C. A., Papayannakos, N., Maschio, G., and Lucchesi, A. (1991). Modelling of the pyrolysis of biomass particles. Studies on kinetics, thermal and heat transfer effects. *Can. J. Chem. Eng.* 69, 907–915. doi:10.1002/cjce.5450690413

Kyzas, G. Z., Deliyanni, E. A., Bikiaris, D. N., and Mitropoulos, A. C. (2018). Graphene composites as dye adsorbents: Review. *Chem. Eng. Res. Des.* 129, 75–88. doi:10.1016/j.cherd.2017.11.006

Lam, K. F., Yeung, K. L., and Mckay, G. (2007). Selective mesoporous adsorbents for and Cu2+ separation. *Microporous Mesoporous Mater.* 100, 191–201. doi:10.1016/j.micromeso.2006.10.037

Lam, S. S., Lee, X. Y., Nam, W. L., Phang, X. Y., Liew, R. K., Yek, P. N., et al. (2018b). Microwave vacuum pyrolysis conversion of waste mushroom substrate into biochar for use as growth medium in mushroom cultivation. *J. Chem. Technol. Biotechnol.* 94 (5), 1406–1415. doi:10.1002/jctb.5897

Lam, S. S., Liew, R. K., Cheng, C. K., Rasit, N., Ooi, C. K., Ma, N. L., et al. (2018a). Pyrolysis production of fruit peel biochar for potential use in treatment of palm oil mill effluent. *J. Environ. Manag.* 213, 400–408. doi:10.1016/j.jenvman.2018.02.092

Lee, S. M., and Tiwari, D. (2012). Organo and inorgano-organo-modified clays in the remediation of aqueous solutions: an overview. *Appl. Clay Sci.* 59-60 (60), 84–102. doi:10.1016/j.clay.2012.02.006

Li, J., Yan, R., Xiao, B., Liang, D. T., and Lee, D. H. (2008). Preparation of nano-NiO particles and evaluation of their catalytic activity in pyrolyzing biomass components†. *Energy Fuels* 22, 16–23. doi:10.1021/ef700283j

Liew, R. K., Chai, C., Yek, P. N. Y., Phang, X. Y., Chong, M. Y., Nam, W. L., et al. (2019). Innovative production of highly porous carbon for industrial effluent remediation via microwave vacuum pyrolysis plus sodium-potassium hydroxide mixture activation. *J. Clean. Prod.* 208, 1436–1445. doi:10.1016/j.jclepro.2018.10.214

Lippens, B., and de Boer, J. H. (1965). Studies on pore systems in catalysts V. The t method. *J. Catal.* 4, 319–323. doi:10.1016/0021-9517(65)90307-6

Litefti, K., Freire, M. S., Stitou, M., and González-Álvarez, J. (2019). Adsorption of an anionic dye (Congo red) from aqueous solutions by pine bark. *Sci. Rep.* 9, 16530–16611. doi:10.1038/s41598-019-53046-z

Liu, S., Ding, Y., Li, P., Diao, K., Tan, X., Lei, F., et al. (2014). Adsorption of the anionic dye Congo red from aqueous solution onto natural zeolites modified with N,N-dimethyl dehydroabietylamine oxide. *Chem. Eng. J.* 248, 135–144. doi:10.1016/j.cej.2014.03.026

Lyubchik, S. B., Benaddi, H., Shapranov, V. V., and Beguin, F. (1997). Activated carbons from chemically treated anthracite. *Carbon* 35, 162–165. doi:10.1016/S0008-6223(97)81121-9

McKay, G., Otterburn, M. S., and Sweeney, A. G. (1980). The removal of colour from effluent using various adsorbents-III. Silica: rate processes. *Water Res.* 14, 15–20. doi:10.1016/0043-1354(80)90037-8

McKay, G. (1996). *Use of adsorbents for the removal of pollutants from wastewaters*. Boca Raton, Florida: CRC Press.

Mizuta, K., Matsumoto, T., Hatate, Y., Nishihara, K., and Nakanishi, T. (2004). Removal of nitrate-nitrogen from drinking water using bamboo powder charcoal. *Bioresour. Technol.* 95, 255–257. doi:10.1016/j.biortech.2004.02.015

Mockovčiaková, A., and Orolínová, Z. (2009). Adsorption properties of modified bentonite clay. *Cheminė Technol.* 1, 47–50.

Molina-Sabio, M., and Rodríguez-Reinoso, F. (2004). Role of chemical activation in the development of carbon porosity. *Colloid. Surface. Physicochem. Eng. Aspect.* 241, 15–25. doi:10.1016/j.colsurfa.2004.04.007

Mui, E. L. K., Cheung, W. H., Lee, V. K. C., and McKay, G. (2008). Kinetic study on bamboo pyrolysis. *Ind. Eng. Chem. Res.* 47, 5710–5722. doi:10.1021/ie070763w

Müller-Hagedorn, M., and Bockhorn, H. (2007). Pyrolytic behaviour of different biomasses (angiosperms) (maize plants, straws, and wood) in low temperature pyrolysis. *J. Anal. Appl. Pyrol.* 79, 136–146. doi:10.1016/j.jaap.2006.12.008

Pütün, A. E., Özbay, N., Önal, E. P., and Pütün, E. (2005). Fixed-bed pyrolysis of cotton stalk for liquid and solid products. *Fuel Process. Technol.* 86, 1207–1219. doi:10.1016/j.fuproc.2004.12.006

Puziy, A. M., Poddubnaya, O. I., Martínez-Alonso, A., Suárez-García, F., and Tascón, J. M. D. (2005). Surface chemistry of phosphorus-containing carbons of lignocellulosic origin. *Carbon* 43, 2857–2868. doi:10.1016/j.carbon.2005.06.014

Qi, W. Y., Hu, C. W., Li, G. Y., Guo, L. H., Yang, Y., Luo, J., et al. (2006). Catalytic pyrolysis of several kinds of bamboos over zeolite NaY. *Green Chem.* 8, 183–190. doi:10.1039/b510602h

Raveendran, K., and Ganesh, A. (1998). Adsorption characteristics and pore-development of biomass-pyrolysis char. *Fuel* 77, 769–781. doi:10.1016/S0016-2361(97)00246-9

Rodríguez-Reinoso, F., and Molina-Sabio, M. (1992). Activated carbons from lignocellulosic materials by chemical and/or physical activation: an overview. *Carbon* 30, 1111–1118. doi:10.1016/0008-6223(92)90143-k

Rodriguez-Reinoso, M., and Ramirez, M. (2013). *Physical recovery of organics from aqueous BFCC product: III. Activated carbon*. Alicante, Spain: Universidad de Alicante; KiOR, Inc.

Rosas, J. M., Berenguer, R., Valero-Romero, M. a. J., RodrÃ-guez-Mirasol, J., and Cordero, T. s. (2014). Preparation of different carbon materials by thermochemical conversion of lignin. *Front. Mater.* 1, 29. doi:10.3389/fmats.2014.00029

Rouquerol, J., and Sing, K. S. W. (1999). *Adsorption by powders and porous solids: principles, methodology and applications*. San Diego, CA: Academic Press.

Ruiz-Rosas, R., García-Mateos, F. J., Gutiérrez, M. d. C., Rodríguez-Mirasol, J., and Cordero, T. (2019). About the role of porosity and surface chemistry of phosphorus-containing activated carbons in the removal of micropollutants. *Front. Mater.* 6, 134. doi:10.3389/fmats.2019.00134

Sadhukhan, A. K., Gupta, P., and Saha, R. K. (2008). Modelling and experimental studies on pyrolysis of biomass particles. *J. Anal. Appl. Pyrol.* 81, 183–192. doi:10.1016/j.jaap.2007.11.007

Scurlock, J. M. O., Dayton, D. C., and Hames, B. (2000). Bamboo: an overlooked biomass resource? *Biomass Bioenergy* 19, 229–244. doi:10.1016/S0961-9534(00)00038-6

Sepulveda, L., Troncoso, F., Contreras, E., and Palma, C. (2008). Competitive adsorption of textile dyes using peat: adsorption equilibrium and kinetic studies in monosolute and bisolute systems. *Environ. Technol.* 29, 947–957. doi:10.1080/09593330802015300

Sharma, R. K., Wooten, J. B., Baliga, V. L., and Hajaligol, M. R. (2001). Characterization of chars from biomass-derived materials: pectin chars. *Fuel* 80, 1825–1836. doi:10.1016/S0016-2361(01)00066-7

Strezov, V., Patterson, M., Zymla, V., Fisher, K., Evans, T. J., and Nelson, P. F. (2007). Fundamental aspects of biomass carbonisation. *J. Anal. Appl. Pyrol.* 79, 91–100. doi:10.1016/j.jaap.2006.10.014

Su, M. H., Azwar, E., Yang, Y., Sonne, C., Yek, P. N. Y., Liew, R. K., et al. (2020). Simultaneous removal of toxic ammonia and lettuce cultivation in aquaponic system using microwave pyrolysis biochar. *J. Hazard Mater.* 396, 122610. doi:10.1016/j.jhazmat.2020.122610

Subba Reddy, Y., Maria Magdalane, C., Kaviyarasu, K., Mola, G. T., Kennedy, J., and Maaza, M. (2018). Equilibrium and kinetic studies of the adsorption of acid blue 9 and Safranin O from aqueous solutions by MgO decked FLG coated Fuller's earth. *J. Phys. Chem. Solid.* 123, 43–51. doi:10.1016/j.jpcs.2018.07.009

The State of the World's Forests 2018 (2018). FAO. Available at: http://www.fao.org/documents/card/en/c/I9535EN/ (Accessed August 20, 2020).

Tonbul, Y. (2008). Pyrolysis of pistachio shell as a biomass. *J. Therm. Anal. Calorim.* 91, 641–647. doi:10.1007/s10973-007-8428-6

Torres-Pérez, J., Soria-Serna, L. A., Solache-Ríos, M., and McKay, G. (2015). One step carbonization/activation process for carbonaceous material preparation from pecan shells for tartrazine removal and regeneration after saturation. *Adsorpt. Sci. Technol.* 33, 895–913. doi:10.1260/0263-6174.33.10.895

Tsai, W. T., Lee, M. K., and Chang, Y. M. (2007). Fast pyrolysis of rice husk: product yields and compositions. *Bioresour. Technol.* 98, 22–28. doi:10.1016/j.biortech.2005.12.005

Valix, M., Cheung, W. H., and McKay, G. (2004). Preparation of activated carbon using low temperature carbonisation and physical activation of high ash raw bagasse for acid dye adsorption. *Chemosphere* 56, 493–501. doi:10.1016/j.chemosphere.2004.04.004

Valix, M., Cheung, W. H., and McKay, G. (2006). Roles of the textural and surface chemical properties of activated carbon in the adsorption of acid blue dye. *Langmuir* 22, 4574–4582. doi:10.1021/la051711j

Valix, M., Cheung, W. H., and Zhang, K. (2008). Role of chemical pre-treatment in the development of super-high surface areas and heteroatom fixation in activated carbons prepared from bagasse. *Microporous Mesoporous Mater.* 116, 513–523. doi:10.1016/j.micromeso.2008.05.020

Wang, S. Y., Tsai, M. H., Lo, S. F., and Tsai, M. J. (2008). Effects of manufacturing conditions on the adsorption capacity of heavy metal ions by Makino bamboo charcoal. *Bioresour. Technol.* 99, 7027–7033. doi:10.1016/j.biortech.2008.01.014

Wang, Z., Saleem, J., Barford, J. P., and McKay, G. (2020). Preparation and characterization of modified rice husks by biological delignification and acetylation for oil spill cleanup. *Environ. Technol.* 41 (15), 1980–1991. doi:10.1080/09593330.2018.1552725

Wasti, A., and Ali Awan, M. (2016). Adsorption of textile dye onto modified immobilized activated alumina. *Journal of the Association of Arab Universities for Basic and Applied Sciences* 20, 26–31. doi:10.1016/j.jaubas.2014.10.001

Yang, R. (2003). *Adsorbents: fundamentals and applications*. New York, NY: John Wiley and Sons.

Yuan, P., Tan, D., and Annabi-Bergaya, F. (2015). Properties and applications of halloysite nanotubes: recent research advances and future prospects. *Appl. Clay Sci.* 112-113, 75–93. doi:10.1016/j.clay.2015.05.001

Zanzi, R., Sjöström, K., and Björnbom, E. (2002). Rapid pyrolysis of agricultural residues at high temperature. *Biomass Bioenergy* 23, 357–366. doi:10.1016/S0961-9534(02)00061-2

Conflict of Interest: The authors declare that the research was conducted in the absence of any commercial or financial relationships that could be construed as a potential conflict of interest.